iScience, Volume *23*

Supplemental Information

PD-L1 Expression Affects Neoantigen Presentation

Masahiro Okada, Kanako Shimizu, Tomonori Iyoda, Shogo Ueda, Jun Shinga, Yoshiki Mochizuki, Takashi Watanabe, Osamu Ohara, and Shin-ichiro Fujii

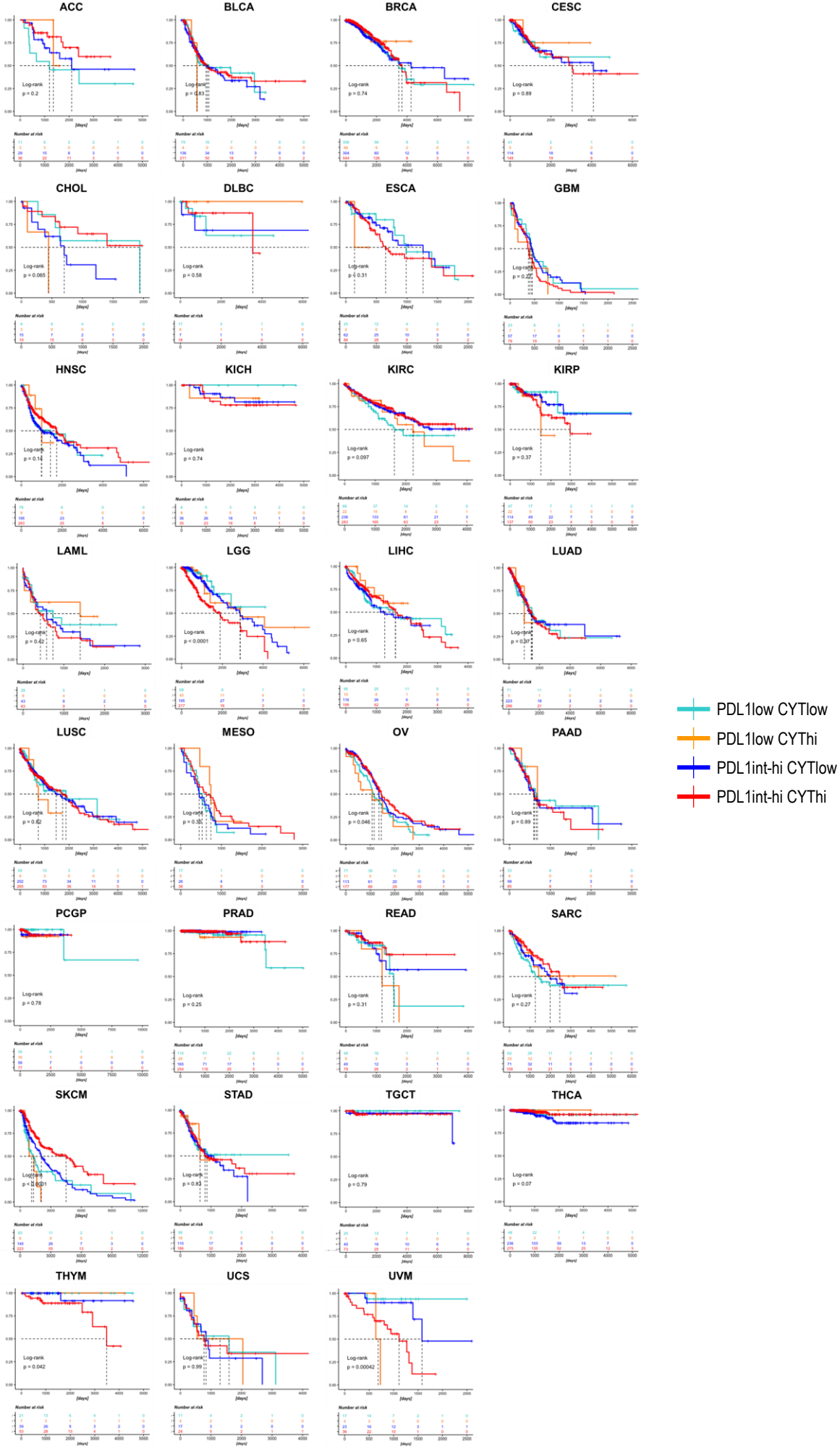

Supplementary Figure 1. TCGA survival analysis focusing on PD-L1 expression with CYT score. Related to Figure 1. Kaplan-Meier survival curves of patients with PD-L1 expression with high versus low CYT score.

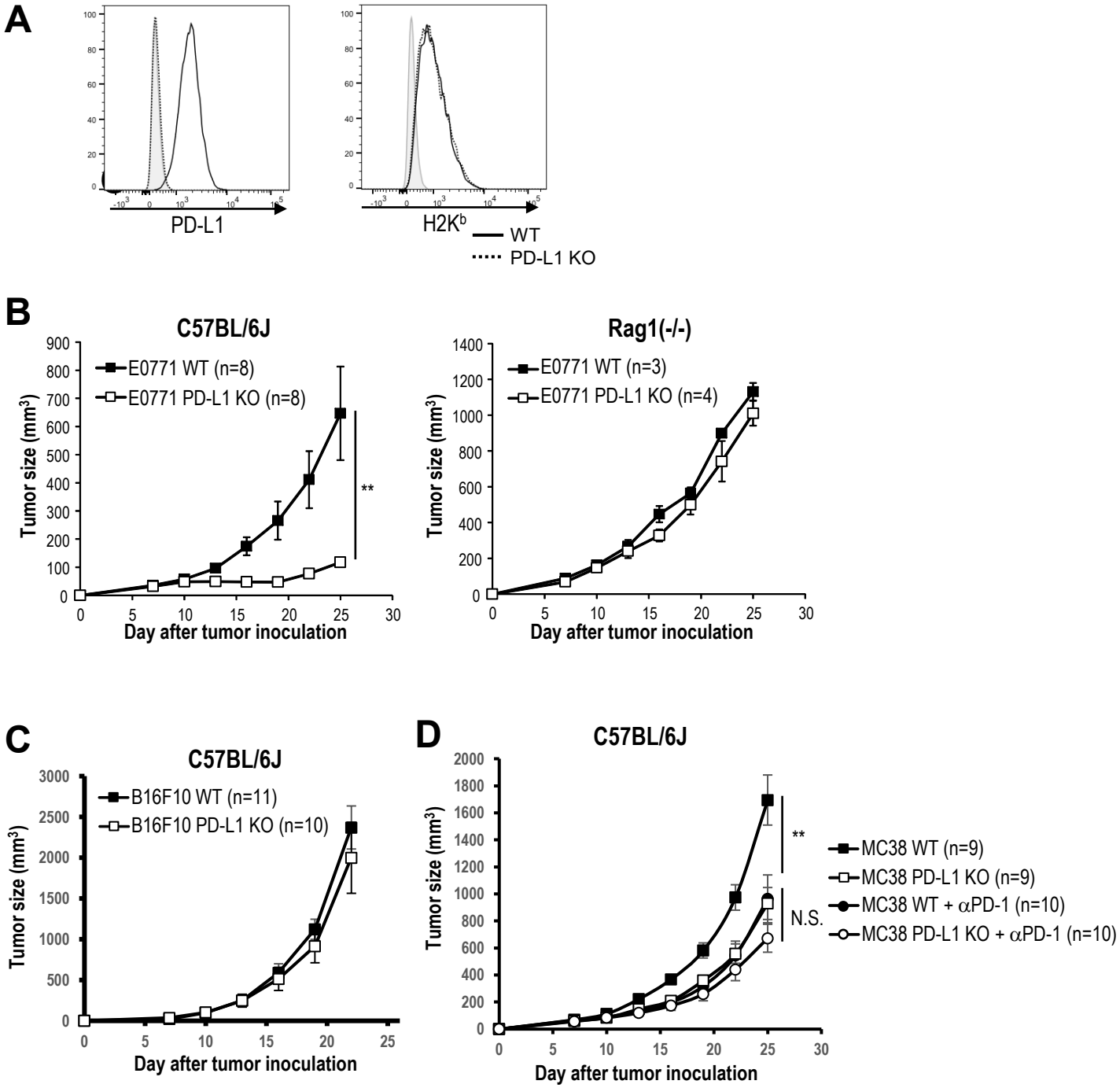

Supplementary Figure 2. Genetic PD-L1 deletion in tumor and effect on antitumor responses. Related to Figure 2.

(A) Flow cytometry analysis of PD-L1 and H-2K^b of MC38-PD-L1-KO cells. **(B)** Tumor growth of E0771 murine breast cancer. C57BL/6J (left) or Rag1$^{-/-}$ (right) mice were subcutaneously (s.c.) injected with 5×10^5 parental or E0771-PD-L1-KO cells, respectively. Tumor growth was monitored at indicated time points by measuring three perpendicular diameters. E0771 and E0771-PD-L1-KO in C57BL/6J mice n = 8/group **$p < 0.01$, in Rag1$^{-/-}$ mice n = 3 and 4/group, respectively; mean ± SEM. **(C)** Tumor growth of B16F10 murine melanoma. Tumor volume was measured every three days from seven days after injection of 1×10^5 parental or B16F10-PD-L1-KO cells in C57BL/6J mice. The values represent mean ± SEM. n = 10 to 11/group. **(D)** Antitumor effect of anti-PD-1 Ab on PD-L1 KO tumor. C57BL/6J mice were s.c. injected with 5×10^5 MC38 or MC38-PD-L1-KO cells and then treated with anti-PD-1 on day 7, 10, and 13. Tumor growth was monitored at indicated time points by measuring three perpendicular diameters. n = 9 to 10/group. Data were analyzed by unpaired Student's t-test, **$p < 0.01$. N.S., non-statistical difference.

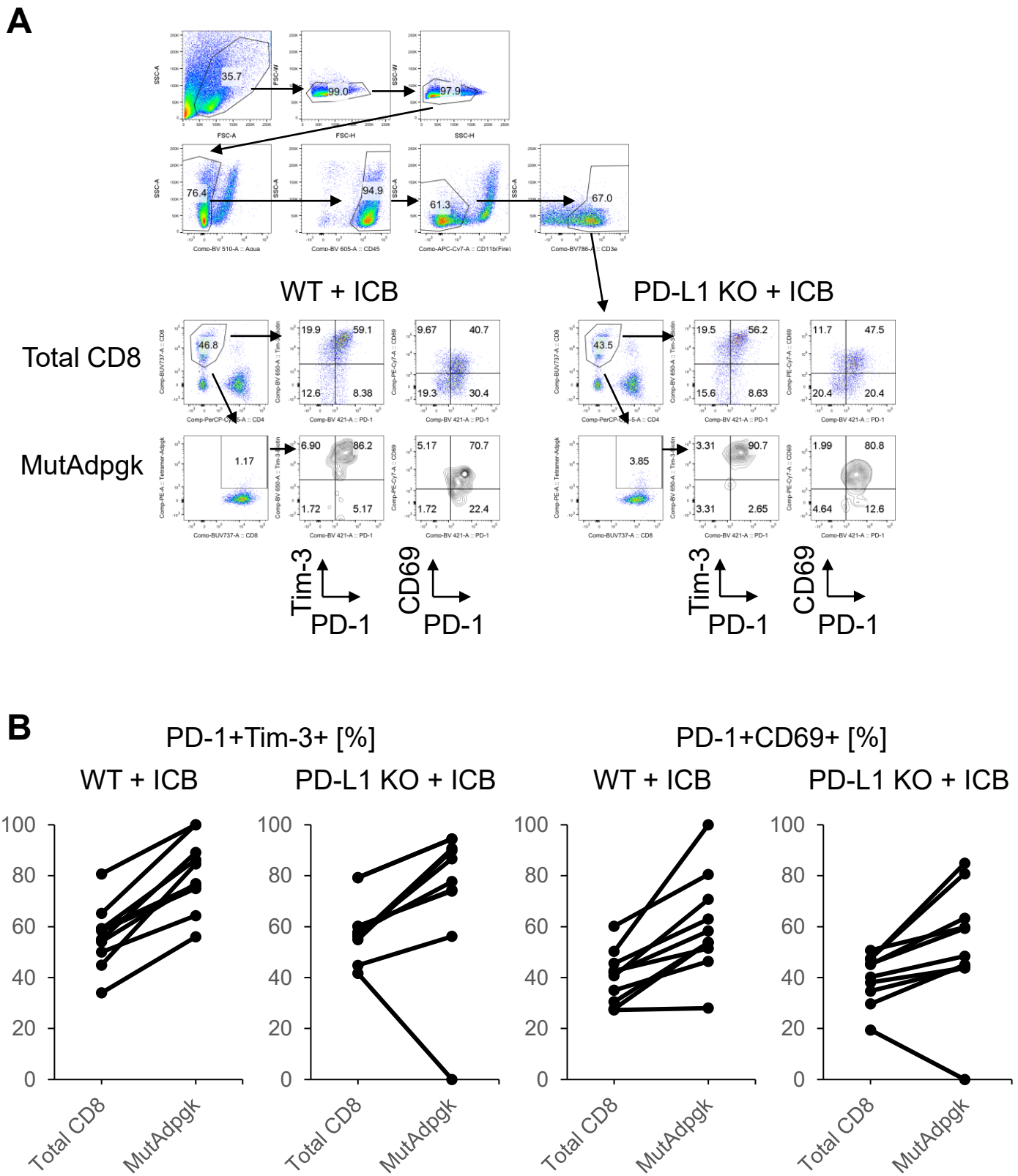

Supplementary Figure 3. Neoantigen specific T cells in tumor infiltrating lymphocytes under ICB therapy. Related to Figure 2.

(A) Gating strategy and representative flowcytometry analysis. **(B)** The percentages of PD-1^{+}Tim-3^{+} or PD-1^{+}CD69^{+} CD8^{+} T cells among total CD8 (non-gated) and MutAdpgk tetramer^{+} cells were plotted. Circles and lines link the respective mice, n=10.

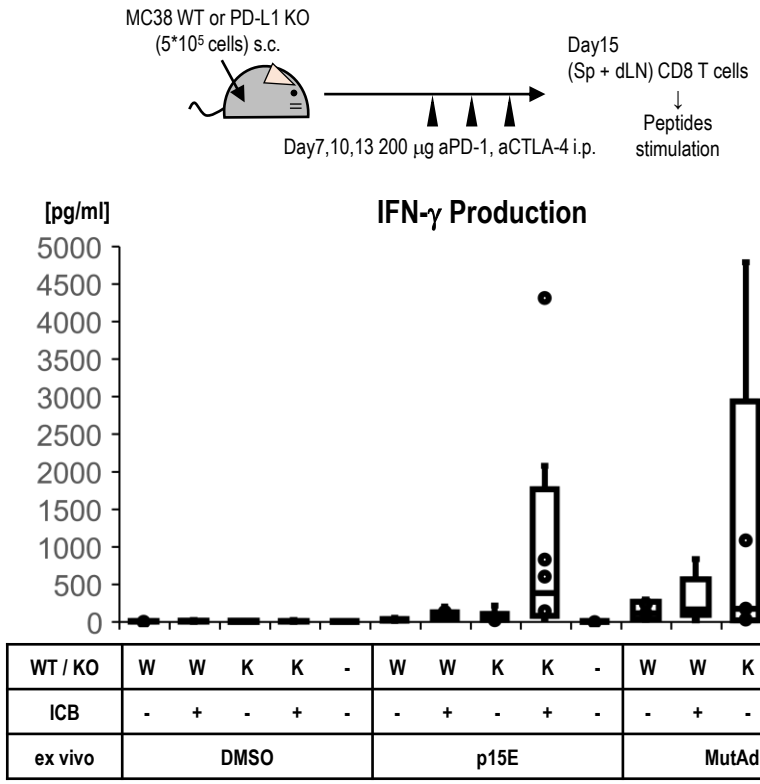

Supplementary Figure 4. Antigen-specific T cell response in ICB-treated mice. Related to Figure 2.
MC38 or MC38-PD-L1-KO tumor-bearing mice were treated with anti-PD-1 and anti-CTLA-4 on day 7, 10, and 13. Fifteen days after tumor inoculation, $CD8^+$ T cells were purified from splenocytes and the tumor draining lymph node, and cocultured with 30 Gy-irradiated splenocytes in the presence or absence of 10 μg/mL p15E or MutAdpgk peptide for 72 h. The culture supernatants were measured for IFN-γ levels by ELISA. Data are pooled from eight or five independent experiments.

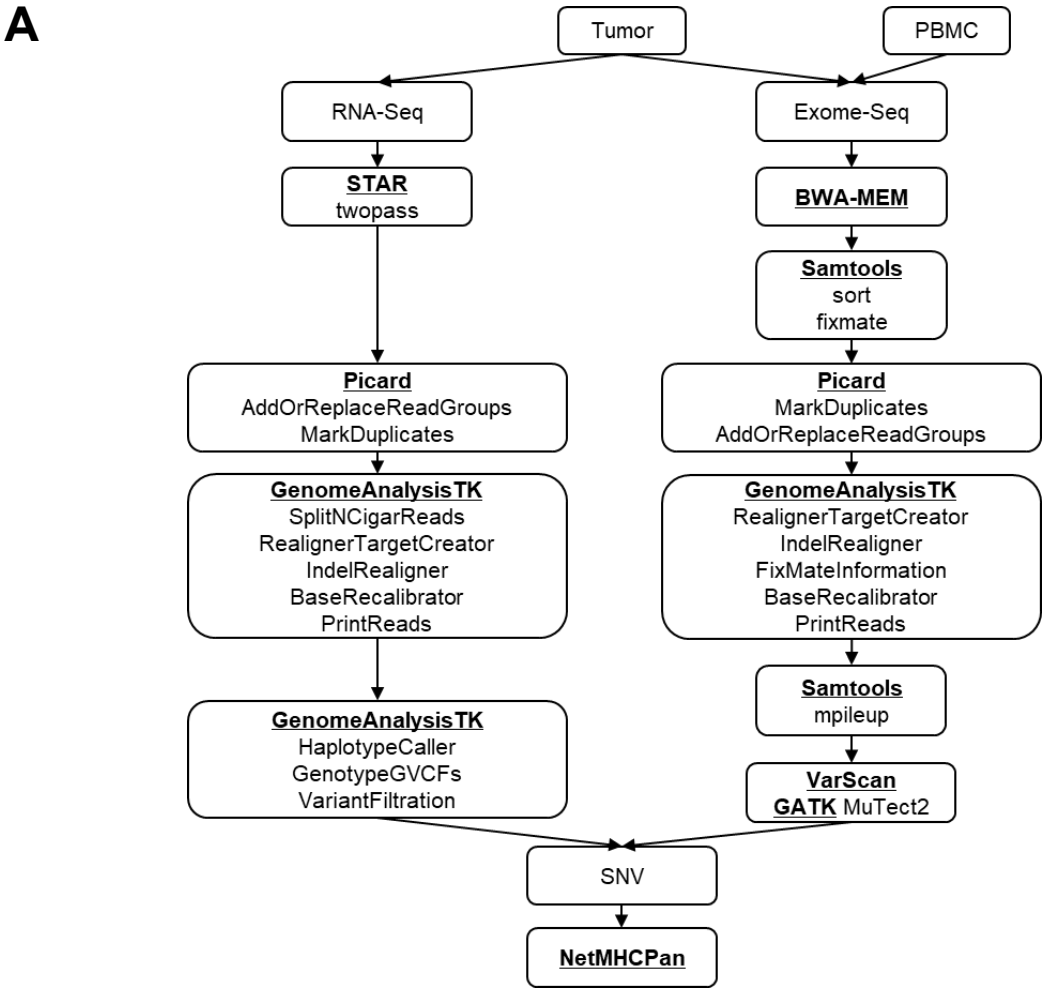

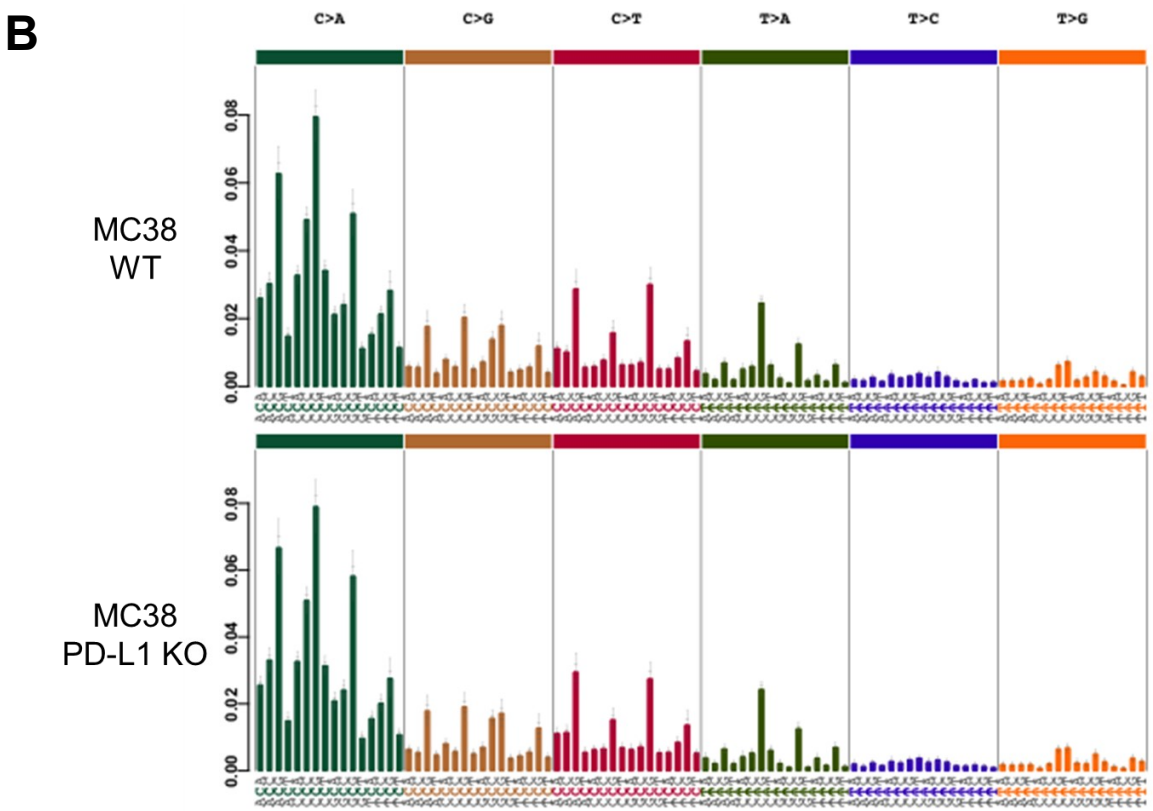

Supplementary Figure 5. Neoantigen identification pipeline. Related to Figure 3.
(A) Mutations in tumors were identified by whole-exome sequence, RNA sequencing, and accompanying bioinformatics approaches using MHC-I-binding algorithms. Reactive peptides sequences and their IC50 values were calculated by NetMHCpan ver3.0. **(B)** Mutation signature analysis of exome sequence from MC38 WT and MC38-PD-L1-KO tumors.

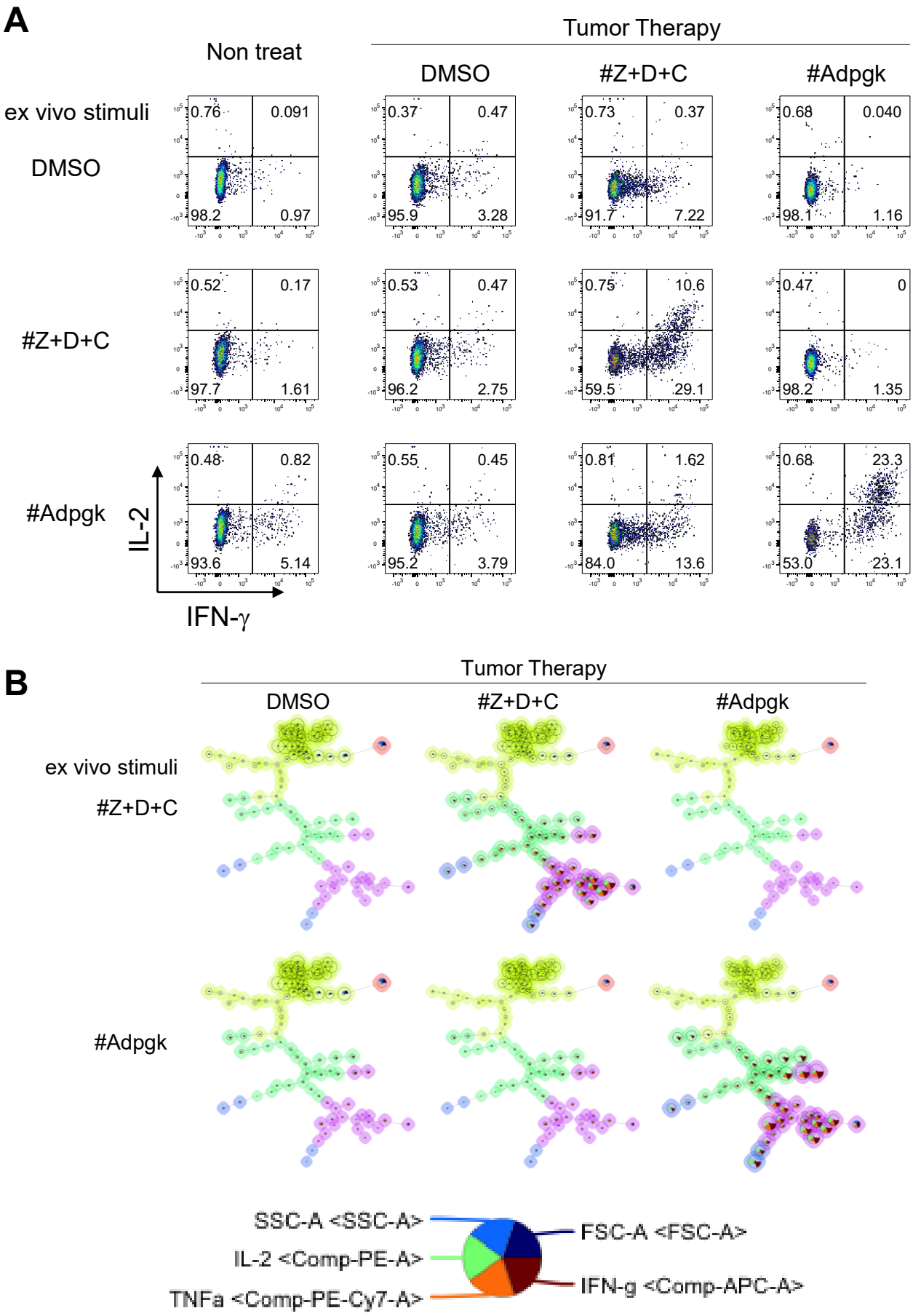

Supplementary Figure 6. Analysis of TIL in mice treated with neoantigen multi-peptides. Related to Figure 6. **(A)** Analysis of TIL in mice treated with neoantigen multi-peptides. TILs from the treated mice were analyzed for cytokine production at day 25. TILs were stimulated by peptides in the presence of anti-CD28 and brefeldin. The frequency of IFN-γ single-producing T cells or IFNγ^{+}IL-2^{+}producing T cells was plotted. Data are pooled from three independent experiments (n = 6). **(B)** FlowSOM analysis representing the multifunctionality of cytokine production in CD8 TILs (IFN-γ^{+}, TNFα^{+} and IL-2^{+}).

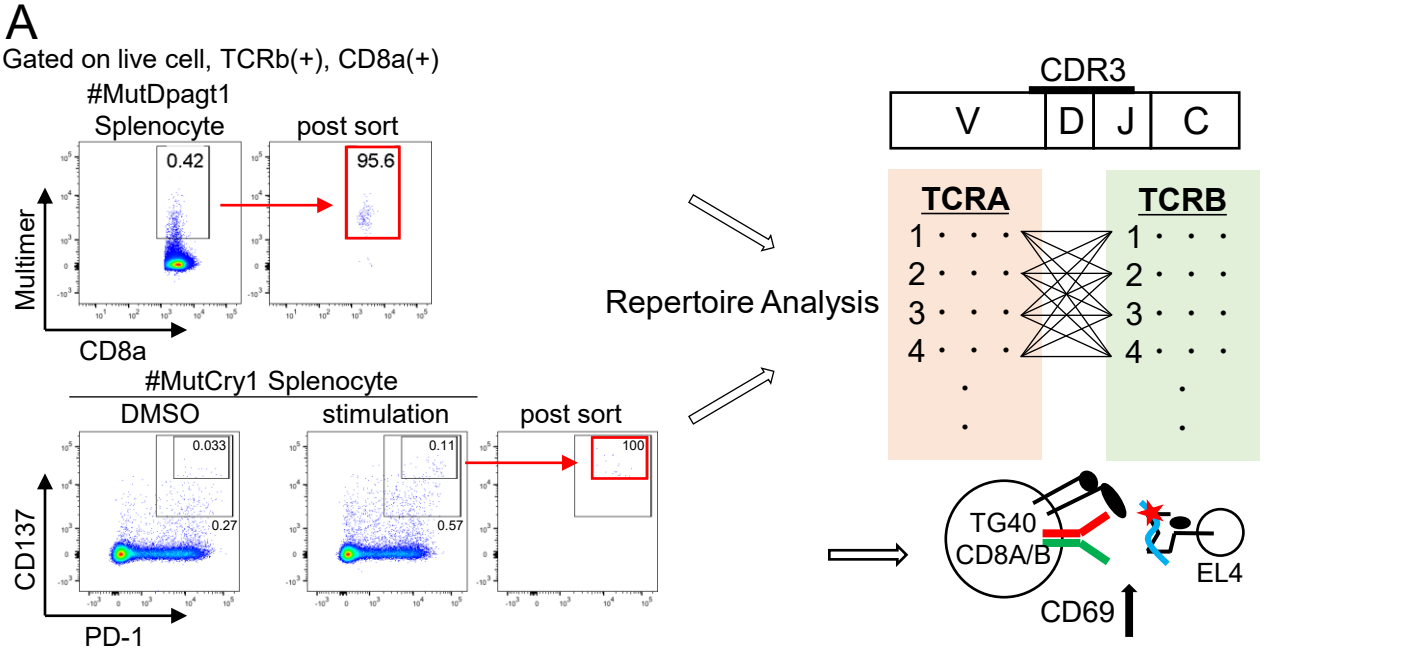

B

Repertoire Top5

#MutDpagt1

TCRA

CDR3 counts	CDR3 Amino Acids Sequence	V gene	D gene	J gene
17964	CATDTNAYKVIF	TRAV8-1*02	-	TRAJ30*01
6854	CATDNMGYKLTF	TRAV8-1*02	-	TRAJ9*01
6088	CAMRDINTGYQNFYF	TRAV16D/DV11*03	-	TRAJ49*01
5484	CAASNMGYKLTF	TRAV7D-2*03	-	TRAJ9*01
4948	CTSETPSPVTLLSTSVQQETGGYKVVF	TRAV7D-2*03	-	TRAJ12*01

TCRB

CDR3 counts	CDR3 Amino Acids Sequence	V gene	D gene	J gene	
15423	CAWRDRGTNTEVFF	TRBV31*01	TRBD1*01	TRBJ1-1*01	
8703	CASSPRTSQNTLYF	TRBV16*01	TRBD2*01	TRBJ2-4*01	
8335	CASSDGGITGQLYF	TRBV13-1*02	TRBD1*01	TRBJ2-2*01	
8067	CASGGTLNTEVFF	TRBV13-2*01	TRBD1*01	TRBJ1-1*01	
6762	CASSLGQLNSDYTF	TRBV12-2*01	TRBD1*01	TRBJ1-2*01	TCR36

#MutCry1

CDR3 counts	CDR3 Amino Acids Sequence	V gene	D gene	J gene
64340	CAASLLNTGNYKYVF	TRAV10*02	-	TRAJ40*01
5262	CAAGGTGYQNFYF	TRAV19*03	-	TRAJ49*01
3521	CALSDPGKLIF	TRAV12N-3*01	-	TRAJ23*01
2657	CALDLMQQGTGSKLSF	TRAV13D-1*02	-	TRAJ58*01
2527	CAVDSGYNKLTF	TRAV7D-2*03	-	TRAJ11*01

CDR3 counts	CDR3 Amino Acids Sequence	V gene	D gene	J gene	
14051	CASSDVEQYF	TRBV13-3*01	TRBD1*01	TRBJ2-7*01	
8496	CASSPDRYEQYF	TRBV16*01	TRBD1*01	TRBJ2-7*01	TCR10
5736	CASSQESWGSSQNTLYF	TRBV2*01	TRBD2*01	TRBJ2-4*01	
5449	CASSQDRGYEQYF	TRBV26*01	TRBD1*01	TRBJ2-7*01	TCR8
4358	CASSPGTFSGNTLYF	TRBV19*01	TRBD1*01	TRBJ1-3*01	

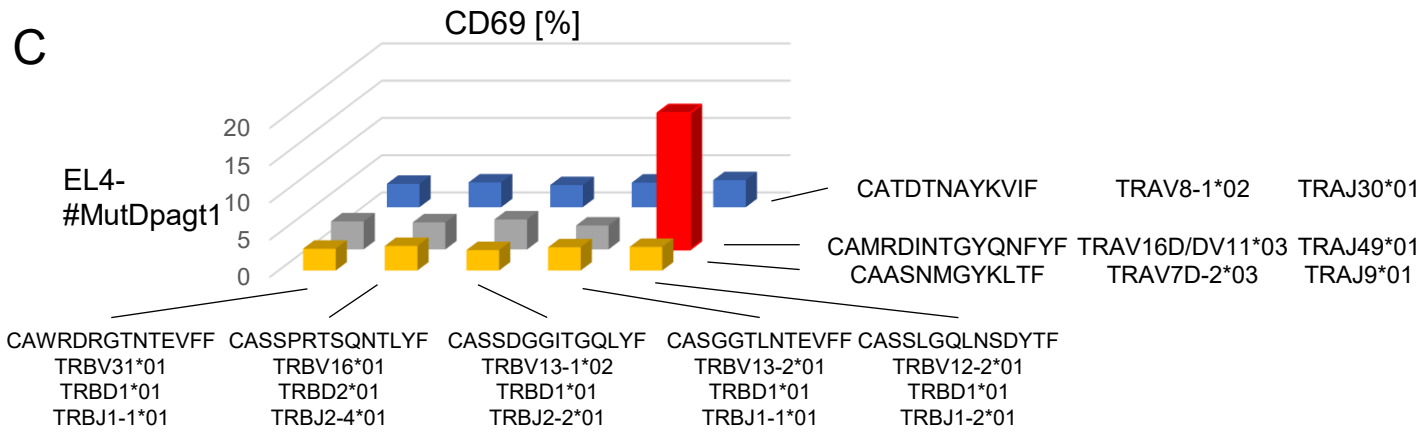

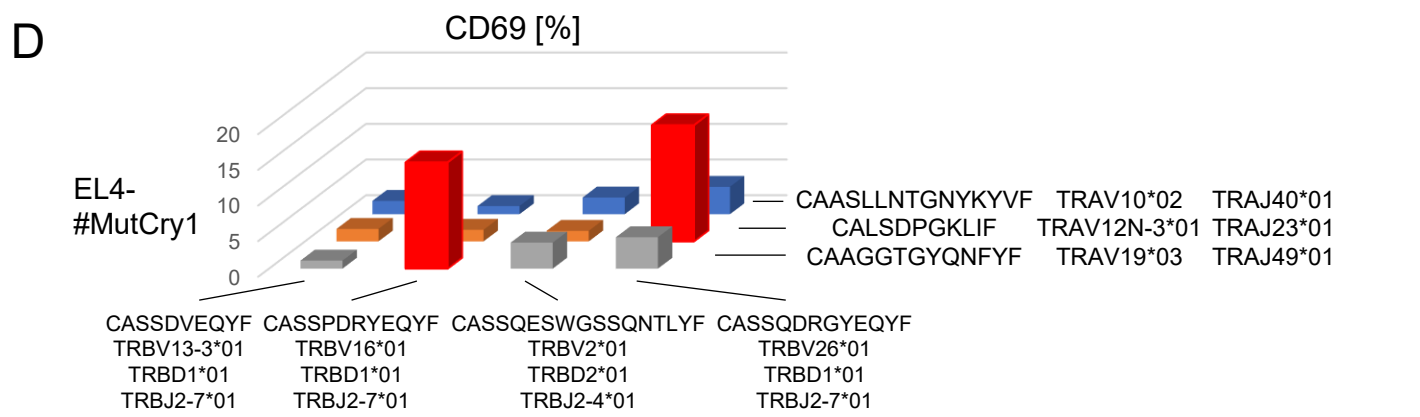

Supplementary Figure 7. Identification of neoantigen-reactive TCR. Related to Figure 7.
(A) Cell sorting of neoantigen-responding CTL. Splenic antigen-specific T cells were isolated as $CD8^+$multimer$^+$ cells for MutDpagt1 and 1-day cultured $CD8^+PD\text{-}1^+CD137^+$ cells for MutCry1 from C57BL/6J mice one week after immunization with neoantigen single peptide (MutDpagt1 or MutCry1) with poly(I:C) and Anti CD40 Abs. Repertoire analyses have been made for each mouse group as shown in the experimental scheme (right). **(B)** Five major TCRα and TCRβ from each group were shown by repertoire analysis. **(C and D)** As shown in the right panel of Fig. S7A, various combinations for TCRα and TCRβ selected from 3–4 major types have been cloned to pMXs-IRES-TdTomato (TCRA) or GFP (TCRB) and transduced to TG40 CD8A/B cells. TG40-bearing TCRA/B (+/+) cells were selected as candidates. Subsequently, these were cocultured with each peptide-pulsed EL4 for 24 h. The percentage of $CD69^+$ cells in TG40 TdTomato/GFP(+/+) cells for MutDpagt1 peptide (C) or MutCry1 peptide (D) is shown. Data are representative of two independent experiments.

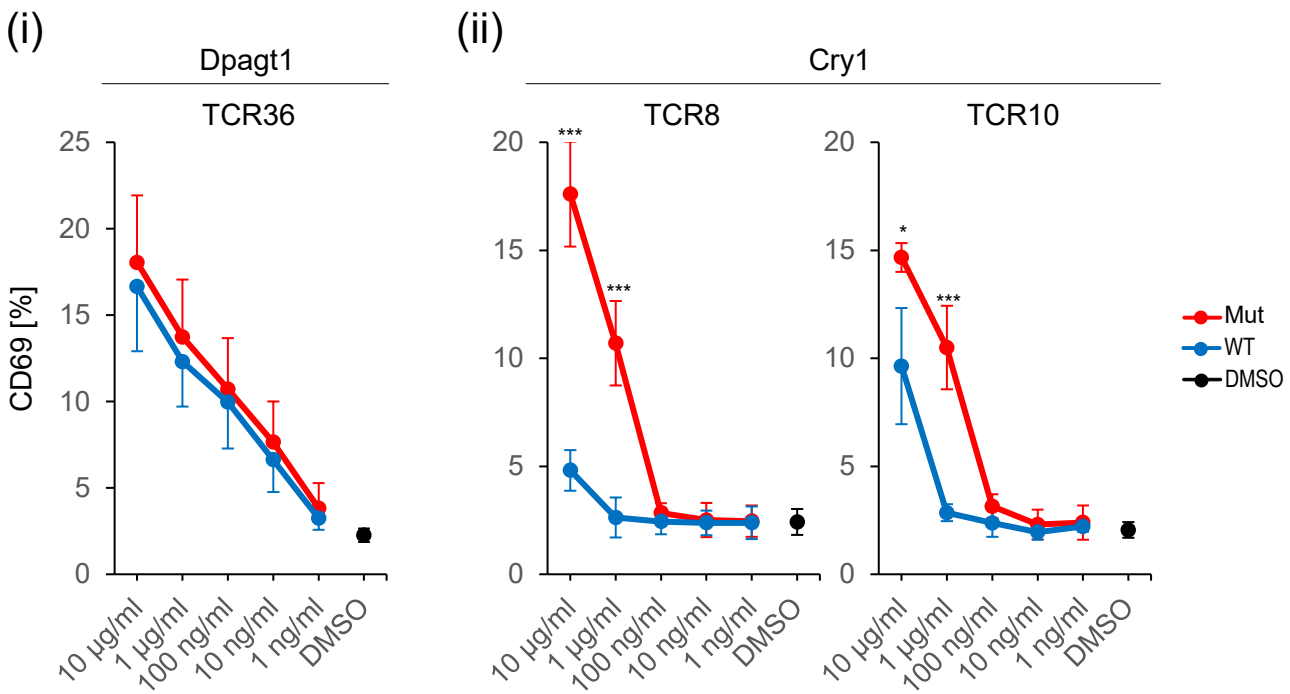

Supplementary Figure 8. Peptide concentration titration of TCRs. Related to Figure 7.
TCR36 (for Dpagt1), TCR8 or TCR10 (for Cry1)-transduced-TG40 cells were cocultured with EL4 in the presence of indicated concentrations of each peptide for 24 h. The percentage of upregulated CD69 of TCR-transduced TG40 cells are shown. Data were pooled from (i) six or (ii) four independent experiments, and the values represent mean ± SD. Data were analyzed by unpaired Student's t-test, *p <0.05, ***p < 0.001.

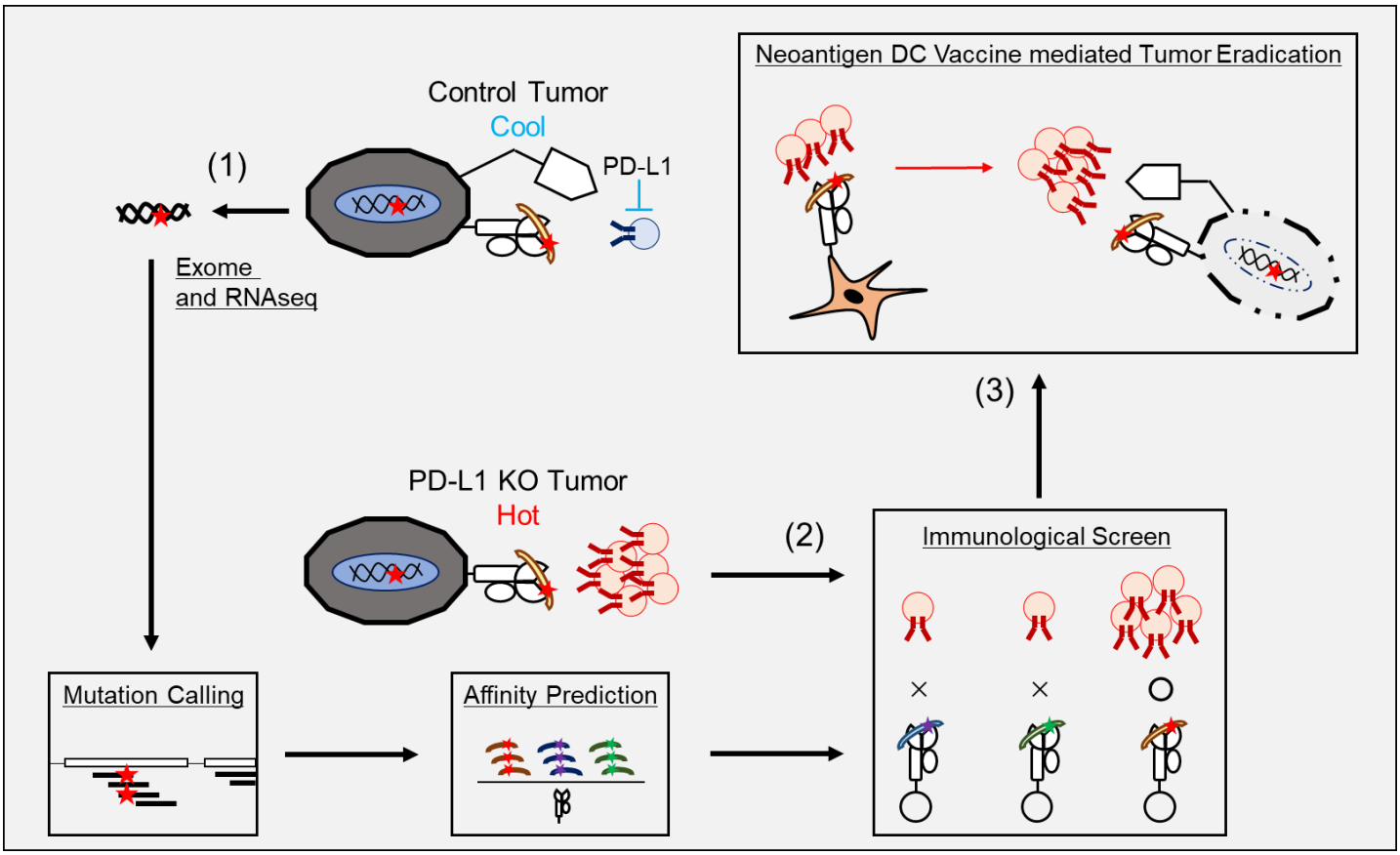

Supplementary Figure 9. Scheme of the study. Related to Figure 2, 3, 5, and 6.
(1) After exome and RNA sequencing, neoantigen candidates were predicted by NetMHCpan. (2) Neoantigens were screened by using activated CTLs from ICB-treated PD-L1 deficient tumor. (3) Vaccination with a mixture of neoantigen-pulsed DCs generated CTLs against PD-L1 positive tumors.

Supplementary Table S1. Neoantigens candidate peptides. Related to Figure 3.

Peptide No	Sequence	IC50(Mut)	Rank(Mut)	Gene Name	Mutation Information	WT Sequence	IC50(WT)
1	KSFHFYCPL	3.3	0.1	Zbtb40	NM_198248 c.G2303C protein-altering (position 768 changed from R to P)	KSFHFYCRL	2.9
2	SNFHFMCAL	6.2	0.1	Kmt2b	NM_001290573 c.G5021T protein-altering (position 1674 changed from R to L)		
3	LSASRYALL	20.7	0.2	Slc12a4	NM_009195 c.G2017T protein-altering (position 673 changed from A to S)		
4	ITIASYIPL	23.4	0.2	Hacd1	NM_013935 c.G648T protein-altering (position 216 changed from M to I)		
5	INFSLQFAL	25	0.2	Pi4kb	NM_001293715 c.G635T protein-altering (position 212 changed from C to F)		
6	RSYQYVMKI	25.3	0.2	Spire1	NM_194355 c.G118T protein-altering (position 40 changed from D to Y)		
7	MSYFLQGTL	26.4	0.2	Copb2	NM_015827 c.A2210C protein-altering (position 737 changed from K to T)		
8	ASYNGFLPV	27.6	0.2	Huwe1	NM_021523 c.C1066A protein-altering (position 356 changed from H to N)		
9	CTFSHLTKL	36.9	0.3	Flrt2	NM_201518 c.G670T protein-altering (position 224 changed from G to C)		
10	KGTLYYYTL	39.5	0.3	Pcsk4	NM_008793 c.C1691A protein-altering (position 564 changed from T to K)		
11	SAMAMFGYM	40.6	0.3	Zbtb8os	NM_025970 c.G167C protein-altering (position 56 changed from C to S)		
12	SSLKSYVQL	42.9	0.3	Ikbkap	NM_026079 c.A943T protein-altering (position 315 changed from T to S)		
13	SAWVPFGGL	43	0.3	Tmem198b	NM_178066 c.G457T protein-altering (position 153 changed from V to F)		
14	ASYSLVAHI	50.7	0.4	Nfe2l2	NM_010902 c.A311T protein-altering (position 104 changed from Q to L)		
15	VQFMSCNLL	51.1	0.4	Taf5l	NM_133966 c.G1717T protein-altering (position 573 changed from A to S)		
16	DVYPFHMIL	52.9	0.4	Gtf3c1	NM_207239 c.A298T protein-altering (position 100 changed from I to F)		
17	KGYRHKVPL	53	0.4	Nsd1	NM_008739 c.A1247T protein-altering (position 416 changed from Q to L)		
18	LMLENYNNL	60.6	0.4	Zfp759	NM_172392 c.G97T protein-altering (position 33 changed from V to L)		
19	SVTVFVNNL	61.7	0.5	Sart3	NM_016926 c.G2126A protein-altering (position 709 changed from S to N)		
20	CVYEHTAVL	62.6	0.5	Herc6	NM_025992 c.G728T protein-altering (position 243 changed from G to V)		
21	RARYFLGNL	69.1	0.5	Dnmt3a	NM_007872 c.G2372T protein-altering (position 791 changed from W to L)		
22	IQPQIYAFL	70.8	0.5	Hace1	NM_172473 c.A2272T protein-altering (position 758 changed from N to Y)		
23	AALTFRRLL	72.4	0.5	Ndufs6	NM_010888 c.T11C protein-altering (position 4 changed from V to A)		
24	KTLTFQGPL	75.2	0.5	Siae	NM_011734 c.A1280C protein-altering (position 427 changed from N to T)		
25	NAFRVYLML	76.9	0.5	Irf2	NM_008391 c.G329T protein-altering (position 110 changed from R to L)		
26	MALSTYYAL	77.7	0.6	Nle1	NM_145431 c.G892T protein-altering (position 298 changed from D to Y)		
27	KNWINYARF	82.7	0.6	Crnkl1	NM_025820 c.G660T protein-altering (position 220 changed from K to N)		
28	FVLESYLNL	83.1	0.6	Rapsn	NM_009023 c.C244G protein-altering (position 82 changed from L to V)		
29	FSLQFALLL	84.4	0.6	Pi4kb	NM_001293715 c.G635T protein-altering (position 212 changed from C to F)		
30	VATINFRRL	86.9	0.6	N4bp2l2	NM_201369 c.G194T protein-altering (position 65 changed from R to L)		
31	FSLSFQHPV	93.2	0.6	Med1	NM_013634 c.G1309T protein-altering (position 437 changed from V to L)		
32	SYIPLFPHL	94.5	0.6	Hacd2	NM_023587 c.G693T protein-altering (position 231 changed from Q to H)		
33	IVAKLIAPL	96.8	0.6	Gcn1l1	NM_172719 c.G4039C protein-altering (position 1347 changed from A to P)		
34	HSFVYSVGF	97.9	0.6	Srebf2	NM_033218 c.G2512T protein-altering (position 838 changed from D to Y)		
35	QIYAFLQGF	108.7	0.6	Hace1	NM_172473 c.A2272T protein-altering (position 758 changed from N to Y)		
36	ASIIVFNLL	118.9	0.6	Dpagt1	NM_007875 c.G637T protein-altering (position 213 changed from V to L)	ASIIVFNLV	609.4
37	SILNWRTKL	142.4	0.7	Ftsj3	NM_025310 c.C922A protein-altering (position 308 changed from L to I)		
38	SAIRSYQYV	146.2	0.7	Spire1	NM_194355 c.G118T protein-altering (position 40 changed from D to Y)		
39	VSRHHRALL	149.5	0.7	Zzef1	NM_001045536 c.G232C protein-altering (position 78 changed from G to R)		
40	YVWGRYDFL	151.4	0.7	Rnpep	NM_145417 c.G864T protein-altering (position 288 changed from L to F)		
41	VIYSECLRV	162.9	0.8	Atm	NM_007499 c.G7036T protein-altering (position 2346 changed from A to S)		
42	QFFHCYCPL	164.7	0.8	Cry1	NM_007771 c.G1246T protein-altering (position 416 changed from V to L)	QFFHCYCPV	781.2
43	IAECTFSHL	176.5	0.8	Flrt2	NM_201518 c.G670T protein-altering (position 224 changed from G to C)		
44	MMKYYYESV	179.6	0.9	Carnmt1	NM_026120 c.G1172C protein-altering (position 391 changed from C to S)		
45	AAALTFRRL	191.5	0.9	Ndufs6	NM_010888 c.T11C protein-altering (position 4 changed from V to A)		
46	SLLEHMSLL	197.4	0.9	Zbtb24	NM_153398 c.A1112T protein-altering (position 371 changed from H to L)		
47	SCRTFLSPL	199.6	0.9	Entpd7	NM_053103 c.G1155C protein-altering (position 385 changed from L to F)		
48	SHYVLYGLI	78.9	0.6	Psmd2	NM_134101 c.G2464A protein-altering (position 822 changed from V to I)		
49	VLYGLIAAM	144.2	0.7	Psmd2	NM_134101 c.G2464A protein-altering (position 822 changed from V to I)		

Transparent Methods

EXPERIMENTAL MODEL AND SUBJECT DETAILS

Mice

Pathogen-free, 6–8 week old C57BL/6J female mice were purchased from Charles River Japan, and Rag1 knockout mice were purchased from The Jackson Laboratory. All mice were maintained under specific pathogen-free conditions. All mice experiments were approved by and performed in compliance with Institutional Animal Care and Use Committee of RIKEN Yokohama Branch.

Reagents

InVivoMAb Anti-mouse PD-1 (RMP1.14) and Anti-mouse CTLA-4 (9D9) were purchased from BioXCell (West Lebanon, NH, USA). H2Kb MuLV p15E peptide (KSPWFTTL) was purchased from MBL (Aichi, Japan).

Flow cytometry

The following monoclonal antibodies (mAbs) were purchased from BD Bioscience, BioLegend, eBioscience, or MBL: anti-CD274 (10F.9G2), anti-H2-K^b (AF6-88.5), anti-CD4 (GK1.5), anti-TCRβ (H57-597), anti-CD8a (53-6.7), anti-TNF-α (MP6-XT22), anti-IL-2 (JES6-5H4), anti-IFN-γ (XMG1.2), anti-CD44 (IM7), anti-CD137 (17B5), anti-CD62L (MEL-14), anti-PD-1 (29F.1A12), anti-CD8 (KT-15), anti-CD3e (145-2C11), anti-CD45 (30-F11), anti-CD8b (YTS156.7.7), anti-CD69 (H1.2F3), anti-CD11b (M1/70), anti-CD366 (RMT3-23), anti-Ly-6C (HK1.4), anti-CD24 (M1/69), anti-Siglec-F (E50-2440), anti-F4/80 (BM8), anti-I-A/I-E (M5/114.15.2), anti-CD103 (2E7), anti-Ly-6G (1A8), anti-CD11c (HL3), anti-CD19 (1D3), anti-CD25 (PC61), anti-NK-1.1 (PK136), anti-CD4 (RM4-5), and anti-FOXP3 (FJK-

16s). H2-D^b Adpgk neoepitope tetramer and H2-K^b Zbtb40 and Dpagt1 neoepitope multimers were purchased from MBL and Immudex (Copenhagen, Denmark), respectively.

Cell culture

MC38 (a kind gift from Dr. MT Lotze, University of Pittsburgh), HEK293T cells and B16F10 cells from ATCC were maintained in Dulbecco's Modified Eagle Medium (DMEM, 4500 mg/L glucose) supplemented with 10% fetal bovine serum (FBS) and 1% penicillin/streptomycin (Gibco). E0771 cells from CH3 BioSystems, EL-4 cells (a kind gift from Dr. Steinman, The Rockefeller University), and TG40 cells expressing CD8A and CD8B (a kind gift from Dr. T Saito, RIKEN) (Yokosuka et al., 2002) were cultured in Roswell Park Memorial Institute (RPMI) 1640 medium supplemented with 10% FBS, 55 μM 2-ME, and 1% penicillin/streptomycin. TG40 cells were constantly sorted to maintain CD8A and CD8B expression at > 95%. Primary T cells were cultured in RPMI-1640 medium supplemented with 10% FBS, 55 μM 2-ME, 1% penicillin/streptomycin, 1% non-essential amino acid solution, and 2 mM L-glutamine. Bone marrow cells were cultured in RPMI-1640 medium supplemented with 5% FBS, 55 μM 2-ME, 1% penicillin/streptomycin, and 1 mM HEPES with GM-CSF Sup derived from J558L-GM-CSF. All cells were cultured in a humid, 5% CO_2, 37°C incubator.

Bone marrow-derived dendritic cell culture and vaccination

Bone marrow-derived DCs were generated in the presence of GM-CSF and matured using LPS on day 6 as previously described (Shimizu et al., 2006). On the following day, mature DCs were harvested and pulsed with 10 μg/mL of indicated peptides for 2 h. After washing with PBS, peptide-pulsed DCs (1×10^6) were intravenously injected for vaccination.

MC38 transplantation mouse model

Briefly, 6 to 10-week-old female mice were shaved on the right flank, and MC38 (1 or 5×10^5 cells) was subcutaneously injected. Tumor volume, calculated as 0.52 × Length × Width × Height [mm^3], was measured at day 7 and every three days. For ICB treatment, 200 μg anti-mouse PD-1 (RMP1.14) and 200 μg anti-mouse CTLA-4 (9D9) were intraperitoneally injected on day 7, 10, and 13. For the CD4 or CD8 T cell-depletion, 250 μg anti-mouse CD4 (GK1.5) or anti-mouse CD8 (53-6.7) were injected intraperitoneally on day -2, 0, 2 and 4, and moreover every 3 to 4 days.

Poly(I:C), anti-CD40 antibody and peptide immunization

10 μg PolyI:C, 30 μg anti-CD40 antibody (1C10) (BioLegend), and 100 μg indicated peptides dissolved in 200 μL PBS were intravenously injected for vaccination (33.3 μg each of peptide #1, #36, and #42 immunization was used) into 6 to 10-week-old female mice. Or 50 μg PolyI:C, 50 μg anti-CD40 antibody, and 100 μg peptide were used for immunization into tumor bearing mice in TCR isolation experiments. 1 week after immunization, splenocytes were further analyzed for multimer staining, intracellular cytokine staining after 6 h culture in the presence of GolgiPlug (BD Bioscience), and activation marker staining and ELISA after 24 h culture with 10 μg/ml peptide.

Neoantigen prediction

Missense mutation-containing amino acid sequences, positioned at 9 in 17 aa, near the first Met, or near the stop codon, were investigated for their potential loading to MHC class I H2-K^b using the NetMHCpan (version 3.0) (Nielsen and Andreatta, 2016) algorithm provided by Immune Epitope DataBase and Analysis Resource (http://tools.iedb.org/mhci/). Predicted peptide length was set as 9 mer. Top 48 candidate peptides (IC50 < 200 nM) were narrowed

down for further biological investigation. Candidate peptides (Table S1) and MutAdpgk (ASMTNMELM) were synthesized (purity > 90%) by GenScript Japan (Tokyo, Japan).

Flow cytometry

Fixable Violet or Aqua Dead Cell stain kit (Invitrogen) was used to eliminate dead cells. Cytokine expression by CD8 T cells was determined using a protocol for intracellular cytokine staining (Shimizu and Fujii, 2009). Briefly, splenic cells were incubated in the presence of Golgi Plug (BD Bioscience) for 6 h with or without 10 μg/mL indicated peptide, followed by incubation with antibodies to the surface markers. Isolated TILs (~1 × 10^6 cells/200 μL) were seeded in 96-well round bottom plates and stimulated with 10 μg/mL indicated peptides and soluble 2 μg/mL anti-CD28 (clone 53.67) (BioLegend) in the presence of GolgiPlug for 6 h. Each 3.3 μg/mL #1, #36, and #42 peptide was used for mixed peptides stimulation. Cells were treated with the anti-mouse CD16/32 antibody (clone 93) (BioLegend) and then stained using cell surface antibodies. Subsequently, the cells were permeabilized in Cytofix-Cytoperm Plus (BD Biosciences) and stained with anti-IFN-γ, -TNF-α, and -IL-2 mAb. Splenocytes (0.5~1 × 10^7 cells) or TILs were treated with anti-mouse CD16/32 antibody in a 50 μL volume, followed by addition of ~10 μL volume of MHC dextramer or MutAdpgk tetramer.

CD69 upregulation assays

TCR retroviruses were transduced into TG40 CD8A/B cells in the presence of 5 μg/mL polybrene (Nacalai) by centrifugation at 2300 rpm for 90 min at 35°C. Further, 2–3 × 10^4 Bulk TG40 cells were cocultured with the same number of EL-4 in the presence or absence of 10 μg/mL corresponding peptides for 24 h in a 96-well flat plate. CD69 upregulation in $TdTomato^+GFP^+$ or GFP^+ cells was analyzed by FACS.

TCR-T assay

MACS-sorted 2×10^5 CD8 T cells were cultured with 2×10^5 mouse CD3/28 beads using the Treg expansion kit (Miltenyi Biotec) and 100 U Immunace (recombinant human IL-2) (Shionogi, Osaka, Japan) in a 24-well plate. Two days after stimulation, TCR retroviruses were transduced into cells in the presence of 6 μg/mL polybrene by centrifugation at 2300 rpm for 90 min at 35°C. On the following day, the cells were harvested and resuspended in fresh medium containing IL-2 after magnetic removal of CD3/28 beads. Two days after transduction, $CD8^+GFP^+$ cells were sorted. Approximately 5×10^4 CD8 T cells were cocultured with 1×10^4 MC38 cells with or without 10 μg/mL peptide for 48 h in the presence of 100 U IL-2 in 96-well flat plates. Culture supernatants were harvested and subjected to IFN-γ ELISA.

TCGA Analysis

Gene expression data (FPKM values) were downloaded from the TCGA GDC portal site (https://portal.gdc.cancer.gov/repository) using gdc-rnaseq-tool (https://github.com/cpreid2/gdc-rnaseq-tool), and clinical data were obtained using R package “TCGAbiolinksGUI" (Silva et al., 2018) on October 2019. FPKM values were converted to TPM values. CYT scores were defined as geomeans of GZMA and PRF1. Overall survival of sub-grouped patients was parsed by R package “survival" and R package “survminer".

Establishment of PD-L1 Knockout cells

gRNA targeting mouse PD-L1 (chr19:29373571-93) expression vector was generated by annealing of oligonucleotides, followed by ligation into BsmBI and BamHI-restricted sites of pCas-Guide-EF1a-GFP (OriGene #GE100018). Primers (forward; gatcgGGCTCCAAAGGACTTGTACGg and reverse;

aaaacCGTACAAGTCCTTTGGAGCCc) were used for construction. CRISPR-Cas9 #PD-L1 vector was transfected into MC38, B16F10, and E0771 cells using the Lipofectamine Plus Reagent and LTX reagent, followed by a medium change to remove the transfection reagents. Three days after transfection, GFP^+ cells were sorted using ARIA3 (BD Biosciences, San Jose, CA, USA) and further cultured. Seven days after transfection, cells were detached using Accutase (Nacalai). Following, PD-L1(-)GFP(-) cells were sorted and further expanded. Several sorting was performed consecutively after expansion to yield completely PD-L1 knockout cells.

IFN-γ ELISA and ELISPOT assay

CD8 T cells were positively selected by mouse CD8a (Ly-2) MicroBeads (Miltenyi Biotec) and MACS LS column. The purity was almost > 90%. For ELISA analysis, 2×10^5 CD8 T cells were MACS purified from the spleen and draining lymph node in tumor-bearing mice, and 2×10^5 30 Gy-irradiated splenocytes were cocultured in the presence of 10 μg/mL peptides in a total volume of 200 μL/well for 72 h. Following, the culture supernatants were harvested and stocked. Technical-duplicate wells were prepared for assays, except the neoantigen peptides screen. IFN-γ production in the frozen and thawed samples were examined using Mouse IFN-γ Duo Set ELISA (R&D systems, Minneapolis, MN, USA) and High Binding Coaster Assay Plates (Corning). ELISPOT assays for antigen-specific IFN-γ secreting cells were performed on 96-well filtration plates (Merck Millipore) coated with rat anti-mouse IFN-γ capture antibody at 10 μg/mL (BD Biosciences R4-6A2) as previously described (Shimizu et al., 2007). Splenic and lymph node CD8 T cells were isolated from immunized mice or naïve mice using $CD8^+$ MACS Beads. Further, 5×10^5 CD8 T cells were cocultured with 3×10^5 irradiated splenic cells pulsed with the indicated peptides for 40–48 h. Biotinylated anti-mouse IFN-γ detection antibody was added at 2 μg/mL (BD Biosciences,

XMG1.2) for 2 h, and spots were developed with Streptavidin-HRP (BD Biosciences) for 1 h and stable DAB substrate (FALMA, Tokyo, Japan). Finally, cells were counted microscopically.

Exome-seq and RNA-seq

MC38 WT and PD-L1 KO tumor tissues were resected and divided into two samples for exome-seq and RNA-seq, then snap frozen in liquid nitrogen. Whole blood was sampled with heparin, and centrifuged PBMCs were prepared for normal tissues. For exome-seq, genomic DNA was extracted using the Wizard Genomic DNA Purification Kit (Promega). DNA was sheared by Covaris (Covaris), and the exome was captured using the SureSelectXT mouse all exon system (Agilent Technologies, 5190-4641) for library preparation. For RNA-seq, RNA was extracted using the Trizol LS Reagent and isolated with chloroform. Following, RNA was precipitated with glycogen and isopropanol, followed by 75% ethanol wash. mRNA was retrieved with oligo dT beads. The RNA sequencing library was prepared using the SureSelect Strand-Specific RNA Library Prep kit (Agilent Technologies, G9691A). Library preparation and pair-end sequencing (100 cycles for RNA sequencing;125 cycles for exome sequencing) on a HiSeq2500 (Illumina) were performed by the Kazusa DNA Research Institute.

Variant calling

Exome-seq data were mapped onto the reference mouse genome (MM9) by BWA-MEM (Li, 2013; Vasimuddin et al., 2019) with default parameters. After removal of unmapped reads, the rest of sequence reads were sorted with a Samtools (Li et al., 2009; Li, 2011). Subsequently, the bam files were processed for removal of PCR duplicates (Picard) and indel realignment, followed by base recalibration referring SNP (number) (GATK) (McKenna et al., 2010). Mutect2 (https://software.broadinstitute.org/ gatk/ documentation/tooldocs/3.8-

0/org_broadinstitute_gatk_tools_walkers_cancer_m2_ MuTect2.php) and VarScan 2 (Koboldt et al., 2012) were used to detect tumor specific variants in comparison with those found by germline blood exome-seq and the variants detected by both of the detection tools were taken as candidate ones in this study. Mutation signature analysis was performed by signeR. RNA-seq data were mapped onto mouse reference genome (MM9) by STAR with two-pass alignment (Dobin et al., 2013). The bam files were processed for removal of PCR duplicates (Picard) and inaccurate spliced reads, and indel realignment, followed by base recalibration referring SNP (number) (GATK). Variants were called using GATK HaplotypeCaller.

T cell receptor repertoire assay

Total RNA was extracted from TrizolLS lysed highly sorted multimer^{+}CD8^{+} T cells or peptide stimulated PD-1^{+}CD137^{+}CD8^{+} T cells and reverse transcribed for first-strand cDNA synthesis using a SMARTer Mouse TCR a/b Profiling kit (Clontech). Both universal mix primer and primers specific for the T cell receptor constant region sequence were used for second-strand amplifications, resulting in TCR PCR products of high purity, which were then submitted for high-throughput DNA sequencing using an Illumina Miseq sequencing system. The sequencing was performed with the paired end (Read1: 300 nt, Read2: 300 nt) using the MiSeq Reagent Kit v3 (MS-102-3003, Illumina). All reads of the TCRα and TCRβ repertoire sequence were analyzed using LymAnalyzer ver1.2.2 (Yu et al., 2016), or randomly extracted 1000 sequences of TCRβ by SeqKit (Shen et al., 2016) were parsed by TCRdist (Dash et al., 2017).

TCR expression vector cloning

The VDJ regions were amplified by PCR using the second PCR products described above as templates, and cloned together with the corresponding C region into pMXs retroviral vectors.

Peptide-reactive pairs of TCRA and TCRB were concatenated with Furin (RAKR)-SGSG-P2A and cloned into pMXs-IRES-GFP. Site-directed mutagenesis was carried out by PCR.

Retrovirus production

pMXs and pCL-Eco were co-transfected into HEK293T cells using FuGene6 (Promega), followed by a medium change to remove the transfection reagents. Virus-containing medium was harvested after 48 h.

WST-1 Assay

Briefly, 1×10^3 MC38 cells were seeded in triplicated well on each 96-well plate before using the Premix WST-1 Cell Proliferation Assay System (Takara Bio Inc, Shiga, Japan) at 24, 48, and 72 h culture. Absorbance was measured after a 1-h incubation. Relative proliferation on day 1 was monitored.

Statistical analysis

Statistical analysis was performed using Microsoft Excel, R, and StatMate. Unpaired student's t-test were used for two experimental groups' comparison. One-way ANOVA followed by Tukey-test were used for multiple experimental groups' comparison. Kaplan-Meier survival curves were analyzed by the log-rank test. P values under 0.05 were considered statistically significant and indicated with *, $p < 0.05$; **, $p < 0.01$; ***, $p < 0.0001$.

KEY RESOURCES TABLE

REAGENT or RESOURCE	SOURCE	IDENTIFIER
Antibodies (for FACS, ELISPOT, Biological Analysis)		
Biotin Mouse IgG1, κ Isotype Ctrl Antibody, MOPC-21	BioLegend	Cat# 400104, RRID:AB_326427
Biotin anti-mouse CD274 (B7-H1, PD-L1) antibody, 10F.9G2	BioLegend	Cat# 124306, RRID:AB_961220
eBioscience™ Streptavidin PE Conjugate	eBioscience™,	Cat# 12-4317-87
Mouse IgG1, kappa Isotype Control, PE Conjugated, Clone MOPC-21 antibody	BioLegend	Cat# 400113, RRID:AB_326435
PE anti-mouse H-2Kb antibody, AF6-88.5	BioLegend	Cat# 116508, RRID:AB_313735
PerCP anti-mouse CD4 antibody, GK1.5	BioLegend	Cat# 100432, RRID:AB_893323
PE/Cy7 anti-mouse TCRb chain antibody, H57-597	BioLegend	Cat# 109222, RRID:AB_893625
APC/Cyanine7 anti-mouse CD8a antibody, 53-6.7	BioLegend	Cat# 100714, RRID:AB_312753
Alexa Fluor® 488 anti-mouse TNF-a antibody, MP6-XT22	BioLegend	Cat# 506313, RRID:AB_493328
PE anti-mouse IL-2 antibody, JES6-5H4	BioLegend	Cat# 503808, RRID:AB_315302
Brilliant Violet 421™ anti-mouse IFN-g antibody, XMG1.2	BioLegend	Cat# 505830, RRID:AB_2563105
Rat Anti-CD44 Monoclonal Antibody, FITC Conjugated, Clone IM7	BD Biosciences	Cat# 553133, RRID:AB_2076224
PE anti-mouse CD137 antibody, 17B5	BioLegend	Cat# 106106, RRID:AB_2287565
CD62L (L-Selectin) Monoclonal Antibody (MEL-14), APC, eBioscience™	Invitrogen	Cat# 17-0621-82, RRID:AB_469410
Brilliant Violet 421™ anti-mouse CD279 (PD-1) antibody, 29F.1A12	BioLegend	Cat# 135221, RRID:AB_2562568
Anti-CD8 (Mouse) mAb-FITC, KT15	MBL	Cat# D271-4, RRID:AB_10597265
FITC anti-mouse CD8a antibody, 53-6.7	BioLegend	Cat# 100706, RRID:AB_312745
CD3e Monoclonal Antibody (145-2C11), PerCP-Cyanine5.5, eBioscience™	Invitrogen	Cat# 45-0031-82, RRID:AB_1107000
BV510 Rat Anti-Mouse CD45, 30-F11	BD Biosciences	Cat# *563891*, *RRID*:AB_2734134
APC Rat Anti-Mouse IFN-γ, XMG1.2	BD Biosciences	Cat# *554413*, *RRID*:AB_398551
PE-Cy™7 Rat Anti-Mouse TNF, MP6-XT22	BD Pharmingen	Cat# *557644*, *RRID*:AB_396761
PerCP/Cyanine5.5 anti-mouse CD8b (Ly-3) antibody, YTS156.7.7	BioLegend	Cat# 126609, RRID:AB_961304
PE/Cy7 anti-mouse CD69 antibody, H1.2F3	BioLegend	Cat# 104512, RRID:AB_493564
Pacific Blue™ anti-mouse CD3e antibody, 145-2C11	BioLegend	Cat# 100334, RRID:AB_2028475
APC/Fire™ 750 anti-mouse/human CD11b antibody, M1/70	BioLegend	Cat# 101262, RRID:AB_2572122
Biotin anti-mouse CD366 (Tim-3) antibody, RMT3-23	BioLegend	Cat# 119720, RRID:AB_2571936
Brilliant Violet 650™ Streptavidin	BioLegend	Cat# 405232
Brilliant Violet 785™ anti-mouse CD3e antibody, 145-2C11	BioLegend	Cat# 100355, RRID:AB_2565969
BV605 Rat Anti-Mouse CD45, 30-F11	BD Biosciences	Cat# *563053*, *RRID*:AB_2737976
BUV395 Rat Anti-Mouse CD44, IM7	BD Biosciences	Cat# *740215*, *RRID*:AB_2739963
BUV737 Rat Anti-Mouse CD8a, 53-6.7	BD Biosciences	Cat# *564297*, *RRID*:AB_2722580
FITC anti-mouse Ly-6C antibody, HK1.4	BioLegend	Cat# 128006, RRID:AB_1186135
PerCP/Cyanine5.5 anti-mouse CD24 antibody, M1/69	BioLegend	Cat# 101824, RRID:AB_1595491
Alexa Fluor® 647 Rat Anti-Mouse Siglec-F, E50-2440	BD Biosciences	Cat# *562680*, *RRID*:AB_2687570
Brilliant Violet 650™ anti-mouse F4/80 antibody, BM8	BioLegend	Cat# 123149, RRID:AB_2564589
Brilliant Violet 785™ anti-mouse I-A/I-E antibody, M5/114.15.2	BioLegend	Cat# 107645, RRID:AB_2565977
PE anti-mouse CD103 antibody, 2E7	BioLegend	Cat# 121406, RRID:AB_1133989
BUV395 Rat Anti-Mouse Ly-6G, 1A8	BD Biosciences	Cat# *563978*, *RRID*:AB_2716852
BUV737 Hamster Anti-Mouse CD11c, HL3	BD Biosciences	Cat# 564986, RRID:AB_2739034
FITC Rat Anti-Mouse CD44, IM7	BD Biosciences	Cat# 553133, RRID:AB_2076224
APC Hamster Anti-Mouse CD3e, 145-2C11	BD Biosciences	Cat# 553066, RRID:AB_398529
APC-Cy™7 Rat Anti-Mouse CD19, 1D3	BD Biosciences	Cat# 557655, RRID:AB_396770
Brilliant Violet 711™ anti-mouse CD25 antibody, PC61	BioLegend	Cat# 102049, RRID:AB_2564130
Brilliant Violet 785™ anti-mouse NK-1.1 antibody, PK136	BioLegend	Cat# 108749, RRID:AB_2564304
PE Rat Anti-Mouse CD62L, MEL-14	BD Biosciences	Cat# *553151*, *RRID*:AB_394666
BUV395 Rat Anti-Mouse CD8a, 53-6.7	*BD* Biosciences	Cat# *563786*, *RRID*:AB_2732919

BUV737 Rat Anti-Mouse CD4, RM4-5	*BD* Biosciences	Cat# *564933*, *RRID*:AB_2732918
FOXP3 Monoclonal Antibody (FJK-16s), PE, eBioscience™	Invitrogen	Cat# 12-5773-82, RRID:AB_465936
H-2D^{b} Adpgk Neoepitope Tetramer-ASMTNMELM-PE	MBL	Cat# TB-5113-1
H-2 Kb/KSFHFYCPL-APC	Immudex	Cat# JD4508-APC (this study)
H-2 Kb/ASIIVFNLL-APC	Immudex	Cat# JD4118-APC (this study)
InVivoMab anti-mouse PD-1 (CD279) antibody, RMP1-14	Bio X Cell	Cat# BE0146, RRID:AB_10949053
InVivoMab anti-mouse CTLA-4 (CD152) antibody, 9D9	Bio X Cell	Cat# BE0164, RRID:AB_10949609
Ultra-LEAF™ Purified anti-mouse CD40 antibody, 1C10	BioLegend	Cat# 102812, RRID:AB_2561489
LEAF™ Purified anti-mouse CD28 antibody, 37.51	BioLegend	Cat# 102112, RRID:AB_312877
Purified anti-mouse CD16/32 antibody, 93	BioLegend	Cat# 101302, RRID:AB_312801
Rat Anti-IFN-gamma Monoclonal Antibody, Unconjugated, Clone R4-6A2	BD Biosciences	Cat# 551216, RRID:AB_394094
Rat Anti-IFN-gamma Monoclonal Antibody, Biotin Conjugated, Clone XMG1.2	BD Biosciences	Cat# 554410, RRID:AB_395374
HRP Streptavidin for ELISPOT	BD Biosciences	Cat# 51-9000209
Biotin anti-mouse CD4 antibody, GK1.5	BioLegend	Cat# 100404, RRID:AB_312689
Biotin anti-mouse CD8a antibody, 53-6.7	BioLegend	Cat# 100704, RRID:AB_312743
Biotin anti-mouse/human CD45R/B220 antibody, RA3-6B2	BioLegend	Cat# 103204, RRID:AB_312989
Biotin anti-mouse I-Ab antibody, AF6-120.1	BioLegend	Cat# 116404, RRID:AB_313723
anti-mouse CD4 (GK1.5)	In Lab	N/A
anti-mouse CD8 (53-6.7)	In Lab	N/A
Chemicals, Peptides, and Recombinant Proteins		
H-2K^{b} MuLV p15E peptide	MBL	Cat# TS-M507-P
H-2D^{b} MutAdpgk Neoepitope ASMTNMELM synthetic peptide	GenScript	N/A (this study)
H-2K^{b} Neoepitope candidates and counterparts synthetic peptides	GenScript	N/A (this study)
LIVE/DEAD™ Fixable Violet Dead Cell Stain Kit, for 405 nm excitation	Invitrogen	Cat# L34964
LIVE/DEAD™ Fixable Aqua Dead Cell Stain Kit, for 405 nm excitation	Invitrogen	Cat# L34966
Collagenase D	Roche	Cat# 11088882001
DNase I	Roche	Cat# 11284932001
Poly(I:C)	TOCRIS	Cat# 4287
BD GolgiPlug™	BD Biosciences	Cat# 555029
Actinomycin D	Sigma	Cat# A1410
Polybrene Solution	Nacalai	Cat# 12996-81
FuGENE® 6 Transfection Reagent	Promega	Cat# E2691
Lipofectamine™ LTX Reagent with PLUS™ Reagent	ThermoFisher	Cat# 15338100
Critical Commercial Assays		
Mouse IFN-gamma DuoSet ELISA	R&D Systems	Cat# DY485-05
SMARTer® Mouse TCR a/b Profiling Kit	TAKARA BIO INC	Cat# Z4404N
Wizard® Genomic DNA Purification Kit	Promega	Cat# A1120
SureSelect XT Mouse All Exon	Agilent	Cat# 5190-4641
SureSelect Strand Specific RNA Reagent Kit	Agilent	Cat# G9691A
Agencourt AMPure XP Kit	Beckman Coulter Genomics	Cat# A63880
TRIzol™ LS Reagent	Invitrogen	Cat# 10296028
BD Cytofix/Cytoperm™	BD Biosciences	Cat# 554714
eBioscience™ Foxp3 / Transcription Factor Staining Buffer Set	Invitrogen	Cat# 00-5523-00
Premix WST-1 Cell Proliferation Assay System	Takara Bio	Cat# MK400
Deposited Data		
C57BL/6J blood Exome-Seq	DDBJ	DRA010264
MC38 WT or PD-L1 KO tumors Exome-Seq	DDBJ	DRA010264
MC38 WT or PD-L1 KO tumors RNA-Seq	DDBJ	DRA010264
TCR Seq for MutDpagt1 and MutCry1	DDBJ	DRA010264

Experimental Models: Cell Lines		
HEK293T	ATCC	Cat# CRL-3216
MC38	Dr. MT Lotze	N/A
EL4	ATCC	Cat# TIB-39
B16F10	ATCC	Cat# CRL-6475
E0771	CH3 BioSystems	Cat# 940001
TG40 mCD8A/mCD8B	Dr. Saito	N/A
Experimental Models: Organisms/Strains		
Mouse: C57BL/6	Charles River Japan	N/A
Mouse: Rag1(-/-)	The Jackson Laboratory	N/A
Recombinant DNA		
pMXs-IRES-GFP Retroviral Expression Vector	Cell Biolabs	Cat# RTV-013
pCas-Guide-EF1a-GFP CRISPR Vector	OriGene	Cat# GE100018
Software and Algorithms		
STAR	Dobin et al., 2013	https://github.com/alexdobin/STAR
NetMHCpan-3.0	Nielsen et al., 2016	http://tools.immuneepitope.org/mhci/
samtools v1.9	Li et al., 2009	http://www.htslib.org/download/
Picard Toolkit v2.20	Broad Institute	https://github.com/broadinstitute/picard
VarScan v2.4	Koboldt et al., 2012	http://dkoboldt.github.io/varscan/
bwa-mem2	Vasimuddin et al., 2019	https://github.com/bwa-mem2/bwa-mem2
bwa v0.7	Li et al., 2009	http://bio-bwa.sourceforge.net/
GATK v3	Broad Institute	https://software.broadinstitute.org/gatk/
ClicO FS	Cheong et al., 2015	clicofs.codoncloud.com
R3.6.1	The R Project	https://www.r-project.org/
RStudio Desktop	RStudio Team	https://rstudio.com/
TCGAbiolinksGUI	Silva et al., 2018	https://bioconductor.org/packages/release/bioc/html/TCGAbiolinksGUI.html
gdc-rnaseq-tool	Dr. Reid	https://github.com/cpreid2/gdc-rnaseq-tool
FlowJo v10.5.3	BD	https://www.flowjo.com/
FlowJo plugins FlowSOM v1.5	Gassen et al., 2015	https://www.flowjo.com/exchange/#/
Excel	Microsoft	https://products.office.com/ja-jp/excel
StatMate V for Win&Mac Hybrid	ATMS Co.,Ltd	http://atms-shop.jp/?pid=64906245
LymAnalyzer_gui v1.2.2	Yu et al., 2016	https://sourceforge.net/projects/lymanalyzer/
TCRdist v0.0.2	Dash et al., 2017	https://github.com/phbradley/tcr-dist
SeqKit v0.8	Shen et al., 2016	https://bioinf.shenwei.me/seqkit/
signeR	Rosales RA et al., 2016	https://bioconductor.org/packages/release/bioc/html/signeR.html

References

Dash, P., Fiore-Gartland, A.J., Hertz, T., Wang, G.C., Sharma, S., Souquette, A., Crawford, J.C., Clemens, E.B., Nguyen, T.H.O., Kedzierska, K., et al. (2017). Quantifiable predictive features define epitope-specific T cell receptor repertoires. Nature *547*, 89-93.

Dobin, A., Davis, C.A., Schlesinger, F., Drenkow, J., Zaleski, C., Jha, S., Batut, P., Chaisson, M. and Gingeras, T.R. (2013). STAR: ultrafast universal RNA-seq aligner. Bioinformatics *29*, 15-21.

Koboldt, D.C., Zhang, Q., Larson, D.E., Shen, D., McLellan, M.D., Lin, L., Miller, C.A., Mardis, E.R., Ding, L. and Wilson, R.K. (2012). VarScan 2: somatic mutation and copy number alteration discovery in cancer by exome sequencing. Genome Res *22*, 568-576.

Li, H. (2011). A statistical framework for SNP calling, mutation discovery, association mapping and population genetical parameter estimation from sequencing data. Bioinformatics *27*, 2987-2993.

Li, H. (2013). Aligning sequence reads, clone sequences and assembly contigs with BWA-MEM. arXiv preprint arXiv:1303.3997.

Li, H., Handsaker, B., Wysoker, A., Fennell, T., Ruan, J., Homer, N., Marth, G., Abecasis, G., Durbin, R. and Genome Project Data Processing, S. (2009). The Sequence Alignment/Map format and SAMtools. Bioinformatics *25*, 2078-2079.

McKenna, A., Hanna, M., Banks, E., Sivachenko, A., Cibulskis, K., Kernytsky, A., Garimella, K., Altshuler, D., Gabriel, S., Daly, M., et al. (2010). The Genome Analysis Toolkit: a MapReduce framework for analyzing next-generation DNA sequencing data. Genome Res *20*, 1297-1303.

Nielsen, M. and Andreatta, M. (2016). NetMHCpan-3.0; improved prediction of binding to MHC class I molecules integrating information from multiple receptor and peptide length datasets. Genome Med *8*, 33.

Shen, W., Le, S., Li, Y. and Hu, F. (2016). SeqKit: A Cross-Platform and Ultrafast Toolkit for FASTA/Q File Manipulation. PLoS One *11*, e0163962.

Shimizu, K. and Fujii, S. (2009). DC therapy induces long-term NK reactivity to tumors via host DC. Eur J Immunol *39*, 457-468.

Shimizu, K., Hidaka, M., Kadowaki, N., Makita, N., Konishi, N., Fujimoto, K., Uchiyama, T., Kawano, F., Taniguchi, M. and Fujii, S. (2006). Evaluation of the function of human invariant NKT cells from cancer patients using α-galactosylceramide-loaded murine dendritic cells. J. Immunol. *177*, 3484-3492.

Shimizu, K., Kurosawa, Y., Taniguchi, M., Steinman, R.M. and Fujii, S. (2007). Cross-presentation of glycolipid from tumor cells loaded with α-galactosylceramide leads to potent and long-lived T cell mediated immunity via dendritic cells. J. Exp. Med. *204*, 2641-2653.

Silva, T.C., Colaprico, A., Olsen, C., Malta, T.M., Bontempi, G., Ceccarelli, M., Berman, B.P. and Noushmehr, H. (2018). Tcgabiolinksgui: a graphical user interface to analyze cancer molecular and clinical data. F1000Research *7*.

Vasimuddin, M., Misra, S., Li, H. and Aluru, S. (2019) Efficient architecture-aware acceleration of BWA-MEM for multicore systems: IEEE. pp. 314-324.

Yokosuka, T., Takase, K., Suzuki, M., Nakagawa, Y., Taki, S., Takahashi, H., Fujisawa, T., Arase, H. and Saito, T. (2002). Predominant role of T cell receptor (TCR)-alpha chain in forming preimmune TCR repertoire revealed by clonal TCR reconstitution system. J Exp Med *195*, 991-1001.

Yu, Y., Ceredig, R. and Seoighe, C. (2016). LymAnalyzer: a tool for comprehensive analysis of next generation sequencing data of T cell receptors and immunoglobulins. Nucleic Acids Res *44*, e31.